Document downloaded from:

http://hdl.handle.net/10251/65982

This paper must be cited as:

Olmeda González, PC.; Tiseira Izaguirre, AO.; Dolz Ruiz, V.; García-Cuevas González, LM. (2015). Uncertainties in power computations in a turbocharger test bench. Measurement. 59:363-371. doi:10.1016/j.measurement.2014.09.055.

The final publication is available at

http://dx.doi.org/10.1016/j.measurement.2014.09.055

Copyright Elsevier

Additional Information

Uncertainties in power computations in a turbocharger test bench

P. Olmeda, A. Tiseira, V. Dolz, L.M. García-Cuevas*

CMT-Motores Térmicos, Universitat Politècnica de València, Valencia 46022, Spain.

Abstract

A specific study of the uncertainties of turbine power output measured in turbocharger test benches is presented using the law of uncertainty propagation and the influence of the different terms that contribute to it is shown. Then, non-linear mixed integer mathematical programming algorithms used with the turbine power uncertainty expression become an essential tool to overcome the problem of selection new sensors to improve an existing test rig or to contribute to a new one. A method of optimisation is presented for two different scenarios: first, where the maximum cost is a constraint; second where the maximum uncertainty is a constraint and the total cost is minimised. When using a large transducers database, computational efforts may be reduced by solving the relaxed non-integer problem by means of sequential quadratic programming and then probing the ceilings and floors of the parameters to get an optimum approximation with low costs. A comparison between the linear uncertainty propagation model and Monte Carlo simulations is also presented, only showing benefits of the later method when computing high order statistical moments of the turbine power output probability distribution.

Keywords: Turbocharger, Uncertainties, Optimisation

1. Introduction

Improving the experimental characterisation of centrifugal compressors and centripetal turbines is a topic of high interest for both researchers and engine manufacturers. To ensure minimum errors in the experimental studies done in turbocharger test rigs, experimental measurement standards [1, 2] are developed and a high technical knowledge and experience in this particular area is needed, as well as high quality experimental facilities. Nevertheless, as both researchers and engine manufacturers are interested into getting experimental results at operating conditions typical of urban driving cycles, the uncertainty of the measurements done within these experimental facilities becomes excessively high for practical purposes and the test rig designer needs to invest in newer equipment.

Although the uncertainty value of every single sensor in a common test rig is generally small, the number of sensors used in such facilities tends to be numerous, each one contributing to the generation of the final uncertainty of the different quantities of interest. The quantification of these uncertainties requires a separate study of parameters such as air temperature, pressure and mass flow and the characteristics of the transducers used to measure them as seen in different works like [3] or [4].

This work shows the variability of the uncertainty, which is studied statistically, as a function of the type of sensors used: thermocouples and resistance temperature detectors used to measure temperature, pressure sensors like piezoelectric and piezoresistive to measure pressure or the air mass flow measured with a hot wire, vortex flowmeter or rotameter. The propagated uncertainty is computed using a first order Taylor expansion of the expressions of interest, then computing the variance-covariance matrix of the obtained linear approximation and neglecting the covariance terms due to lack of correlation between the different variables, and assuming normal distribution of the final results. While there are several papers about turbocharger experimental studies with uncertainties computations done in detail, like in [5], it is usually not the case. The aim of this work is the development of a flexible methodology to estimate the measurement uncertainties in the particular case of the experimental characterisation of turbochargers and to give hints to the test rig designer to select new trans-

*Corresponding author. Tel: +34963877650; fax: +34963877659
Email address: luiga12@mot.upv.es (L.M. García-Cuevas)
URL: www.cmt.upv.es (L.M. García-Cuevas)

ducers optimising the results with a minimum cost.

As usual in this sort of works, it is supposed that the tests are being conducted in almost-adiabatic conditions in a cold test rig. Povedin et al. [6] analyse the influence of different parameters of lubricating oil in the performance of radial turbochargers in almost-adiabatic conditions and it is said that the uncertainty of the measurement can be very problematic at low operating conditions, but no computation of these uncertainties is done. Some authors make their tests in hot conditions. Serrano et al. [7] propose a thermal characterisation methodology successfully applied in a turbocharger, but no uncertainties are quantified. T. Thurnheer et al. [8], present an experimental investigation on different injection strategies in a heavy-duty diesel engine and the uncertainty of different measurements is shown but no propagation is done. M. Tancrez et al. [9] present a new representation of the turbine performance maps oriented for turbocharger characterisation and it is said when using some representations of turbine maps in numerical simulations the uncertainties of the measurements can propagate very amplified to the final results, so it is very important to quantify them. In the work presented by P. Günther et al. [10] the deformation and the movement of a high speed rotor is measured and the uncertainties involved are quantified. The authors suggest to calculate the propagation of uncertainties in order to understand how the results can be affected by the propagation effect. Therefore, through this work it is possible to obtain more robust results thanks to the calculus applied to the propagation of uncertainties combined with the sensors selection. In order to optimally select new sensors, a non-linear integer programming problem has to be solved. Several techniques are used in real-world engineering problems involving non-linear programming, as in the work of Weihong Zhang et al. [11], and non-linear integer programming, as can be seen in the work of Daisuke Yokoya [12], Sahoo, N. P. [13] or Pal, P [14]. Rose applies an optimisation process to design of experiments to minimise the effect of measurement uncertainties [15]. This work presents one technique suitable for the selection of new experimental equipment in turbocharger gas stands.

This paper is divided in four parts: in the first part the basic equations of uncertainties propagation are presented and the expression for the turbine power uncertainty is developed; in the second part an optimisation methodology to select transducers for a turbocharger test rig is explained; in the third part, the turbine power uncertainty obtained during a typical experimental campaign is shown and compared with the results of Monte Carlo simulations and an optimisation process to select new testing equipment is exposed; last, conclusions and hints to achieve better results are presented.

2. Propagation of uncertainty

Uncertainty in direct measurements is propagated to derived quantities that are of interest such as compressor power or turbine efficiency. To assess the reliability of the measurements of physical quantities, values of their uncertainties should be given in a standardized way. There are different types of methods used to estimate the distribution of the probability density of values of uncertainty for a multivariate system, some of them comprise "Bootstrapping" and "Monte Carlo" methodologies. A good alternative is described in [16] by the Joint Committee for Guides in Metrology and is applied in this work. The objective focuses on finding the standard deviation but not the probability density of the results. Moreover, the bootstrapping and Monte Carlo [17] methods require more computational time than the standard method but generate more information.

Standard deviation is used as a measure of uncertainty, and some information about the probability density function that describes the behaviour of the measurements done by means of each transducer is needed to compute it using manufacturer's data. When there is no information available about the expected probability density function, an uniform distribution should be used.

In the present work, a coverage factor k is used on the basis of a level of confidence of 99.7 % of the real values of the measurands falling inside an interval $z - k \cdot u_z$ to $z + k \cdot u_z$, what gives $k = 3$ in case of normal distributions. In the case of uniform distributions, the real values of the measurands fall inside the interval $z - \sqrt{3} \cdot u_z$ to $z + \sqrt{3} \cdot u_z$ with a level of confidence of 100 %. The value $k \cdot u_z$ is called expanded uncertainty. The standard uncertainty of z, where z is the estimate of the measurand Z and thus the result of the measurement, is obtained by appropriately combining the standard uncertainties of the input estimates $x_1, x_2, ..., x_n$. This combined standard uncertainty of the estimate z is denoted by u_z.

For a given derived quantity z, its uncertainty u_z can be computed as:

$$u_z^2 = \sum_i^n \left(\frac{\partial z}{\partial x_i} \right)^2 u_{x_i}^2, \tag{1}$$

where, again u_{x_i} is the uncertainty of the variable x_i and it is assumed that there is no correlation between the measurements. This can be also approximated by:

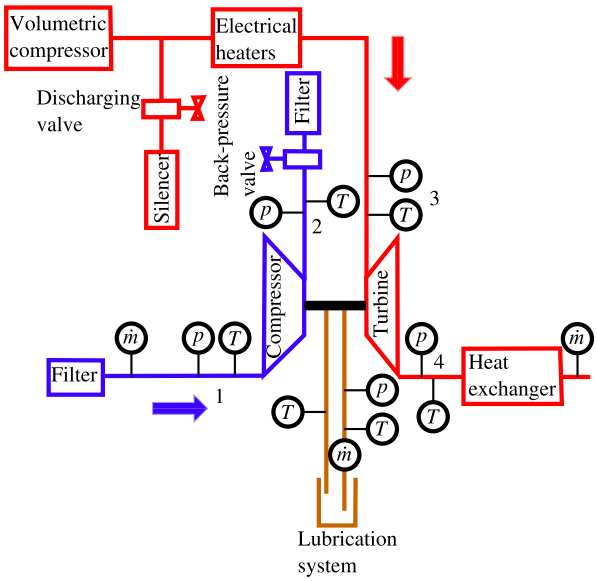

Figure 1: Typical turbocharger test rig arrangement

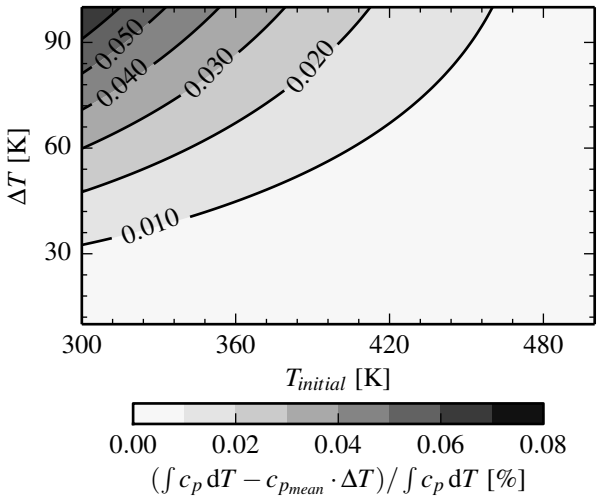

Figure 2: $\frac{\int c_p \,\mathrm{d}\,T - c_p(T_{mean}) \cdot \Delta T}{\int c_p \,\mathrm{d}\,T}$, being $T_{mean} = T_{initial} + \frac{\Delta T}{2}$

$$u_z^2 = \sum_i^n \frac{1}{4}[f(x_1, \ldots, x_{i-1}, x_i + u_{x_i}, x_{i+1}, \ldots, x_n) - f(x_1, \ldots, x_{i-1}, x_i - u_{x_i}, x_{i+1}, \ldots, x_n)]^2 \quad (2)$$

3. Experimental application in turbine power

In this section, the uncertainty associated to the computation of the power output of a turbine in a turbocharger test rig is presented. The influence of several terms is estimated.

A typical test rig arrangement is schematically shown in Figure 1.

In many cases, tests are done in almost-adiabatic conditions, so the heat flow can be neglected and the power output of the turbine can be computed as:

$$\dot{W}_t \simeq \dot{m} \int_{T_{03}}^{T_{04}} c_p \,\mathrm{d}\,T \quad (3)$$

Doing the tests in a cold test rig in almost-adiabatic conditions is very common because heat transfer between the different parts of the turbocharger and to the atmosphere is almost trivially measurable. Payri et al [18] and Serrano et al [19] use this technique to characterise mechanical losses in small turbochargers. Povedin et al [6] show the influence of several parameters of the lubricating oil in the performance of a centrifugal compressor is measured also in quasi-adiabatic conditions. Nevertheless, some authors try to model the heat transfer, like Bohn et al [20] and Serrano et al [21], throwing interesting results, as can be a methodology to separate turbine power from heat transfer in measurements done in hot test rigs.

Equation 3 can be further simplified:

$$\dot{W}_t \simeq \dot{m} c_p\,(T_{mean}) \cdot (T_{04} - T_{03}) \quad (4)$$

where $T_{mean} = \frac{T_{03}+T_{04}}{2}$.

As can be seen in Figure 2, the systematic error incurred by approximating the integral is negligible.

Generally, the only directly measured variable in equation 4 is the mass flow rate: the specific heat capacity is obtained from correlations and the total temperature is approximated by measuring the static temperature plus the kinetic energy contribution multiplied by a recovery factor. Following, the different terms are to be discussed:

3.1. Total temperature

The total temperature T_0 is:

$$T_0 = T \cdot \left(1 + \frac{\gamma - 1}{2} M^2\right) \quad (5)$$

where T is the static temperature, γ is the heat capacity ratio of the air and M is the Mach number.

The measured temperature $\hat{T}$ lies between the static and the total temperature, as can be seen in [22]. A recovery factor e as described in [23] can be used:

$$e = \frac{\hat{T} - T}{T_0 - T} = \frac{\hat{T}/T - 1}{\frac{\gamma-1}{2}M^2} \tag{6}$$

The measured temperature is, therefore:

$$\hat{T} = T \cdot \left(1 + \frac{\gamma - 1}{2} e M^2\right) \tag{7}$$

Using equations 5 and 7, the total temperature becomes:

$$T_0 = \hat{T} + (1 - e)\frac{\gamma - 1}{2} T M^2 \tag{8}$$

If the Mach number is not very high:

$$T_0 \simeq \hat{T} + (1 - e)\frac{\gamma - 1}{2}\frac{\dot{m}^2 R \hat{T}^2}{\gamma p^2 A^2} \tag{9}$$

where γ is a function of the static temperature and the composition of the air and R is only a function of the composition of the air. When working with air, its more important differences in composition are due to variations in its specific humidity; other species could be needed in some cases, i.e., when working with exhaust gases.

u_{T_0} can be computed:

$$\begin{aligned} u_{T_0}^2 \simeq & \left[1 + (1 - e)(\gamma - 1)\frac{\dot{m}^2 R \hat{T}}{\gamma p^2 A^2}\right]^2 \cdot u_{\hat{T}}^2 \\ & + \left[\frac{\gamma - 1}{2}\frac{\dot{m}^2 R \hat{T}^2}{\gamma p^2 A}\right]^2 \cdot u_e^2 \\ & + \left[(1 - e)(\gamma - 1)\frac{\dot{m} R \hat{T}^2}{\gamma p^2 A^2}\right]^2 \cdot {u_{\dot{m}}}^2 \\ & + \left[(1 - e)(\gamma - 1)\frac{\dot{m}^2 R \hat{T}^2}{\gamma p^3 A^2}\right]^2 \cdot {u_p}^2 \\ & + \left[(1 - e)(\gamma - 1)\frac{\dot{m}^2 R \hat{T}^2}{\gamma p^2 A^3}\right]^2 \cdot {u_A}^2 \\ & + \left[(1 - e)\frac{\gamma - 1}{2}\frac{\dot{m}^2 \hat{T}^2}{\gamma p^2 A^2}\right]^2 \left(\frac{\mathrm{d}R}{\mathrm{d}Y}\right)^2 \cdot {u_Y}^2 \\ & + \left[(1 - e)\frac{\dot{m}^2 R \hat{T}^2}{2\gamma p^2 A^2} - (1 - e)\frac{\gamma - 1}{2}\frac{\dot{m}^2 R \hat{T}^2}{\gamma^2 p^2 A^2}\right]^2 \\ & \cdot \left[\left(\frac{\partial \gamma}{\partial Y}\right)^2 \cdot {u_Y}^2 + \left(\frac{\partial \gamma}{\partial \hat{T}}\right)^2 \cdot {u_{\hat{T}}}^2\right] \end{aligned} \tag{10}$$

Considering a low Mach number (below 0.3) inside the ducts is consistent with the measurements done by the authors of this paper and gives a systematic error in the computation of T_0 of less than 0.1 K in the worst cases, being it below 0.01 K in the majority of the points studied. If not assuming the hypotesis of low Mach number, the expression of u_{T_0} becomes more complex while not giving an important improvement in accuracy and affecting the computational time used during the optimisation process explained later in this work.

3.2. Specific heat capacity

The specific heat capacity c_p is a function of the temperature and the composition of the air, which, as commented before, is computed using its specific humidity:

$$c_{p_{mean}} = c_p\left(T_{mean}, Y\right) = c_p\left(\frac{T_{03} + T_{04}}{2}, Y\right) \tag{11}$$

Its uncertainty is:

$$\begin{aligned} u_{c_{p_{mean}}}^2 = & \left(\frac{\partial c_{p_{mean}}}{\partial T}\right)^2 \cdot \frac{u_{T_{03}}^2}{2} + \left(\frac{\partial c_{p_{mean}}}{\partial T}\right)^2 \cdot \frac{u_{T_{04}}^2}{2} \\ & + \left(\frac{\partial c_{p_{mean}}}{\partial Y}\right)^2 \cdot u_Y^2 \end{aligned} \tag{12}$$

where $u_{T_{03}}$ and $u_{T_{04}}$ can be obtained using equation 10.

3.3. Turbine power uncertainty

The turbine power uncertainty can be computed as:

$$\begin{aligned} u_{\dot{W}_t}^2 = & \left[c_{p_{mean}} \cdot (T_{03} - T_{04})\right]^2 \cdot u_{\dot{m}}^2 \\ & + \left(\dot{m}\frac{\partial c_{p_{mean}}}{\partial Y}\right)^2 \cdot u_Y^2 \\ & + \left[\left(\dot{m}\frac{\partial c_{p_{mean}}}{2\partial T}\right)^2 \cdot (T_{03} - T_{04})^2 \right. \\ & \left. + \left(\dot{m} \cdot c_{p_{mean}}\right)^2\right] \cdot \left(u_{T_{03}}^2 + u_{T_{04}}^2\right) \end{aligned} \tag{13}$$

where $u_{T_{03}}$ and $u_{T_{04}}$ can be obtained from equation 10. If several sensors for a given value are used, the uncertainty associated to its mean value is to be used. For example, in the case of several mass flow rate sensors:

$$u_{\dot{m}} = \sqrt{\sum_i^{N_{\dot{m}}} \left(\frac{u_{\dot{m}_i}}{N_{\dot{m}}}\right)^2} \tag{14}$$

where $N_{\dot{m}}$ is the number of mass flow rate sensors used.

4. Optimisation methodology

In order to optimise the investment in new experimental equipment, a database of prices and technical specifications of sensors from different suppliers has to be compiled. Also, the expression of turbine output power uncertainty and a representative experimental dataset are needed. After that, the test rig designer has one of the next targets:

- Minimise the uncertainty for a given maximum acceptable economic cost.
- Minimise the cost for a given target uncertainty.

In the former case, the cost is a constraint of the optimisation problem and the uncertainty is weighted so it is more important to reduce it in some zone of interest, whereas in the latter the cost is the objective function to optimise.

The first case can be described as:

$$\begin{aligned} \underset{y}{\text{minimise}} \quad & f\left(u_{\dot{W}_t}(y)\right) \\ \text{subject to} \quad & \sum_{i}^{n} d_i \cdot H(y_i - y_{i,s}) \cdot (y_i - y_{i,s}) \leq d_M \\ & 0 \leq y_i \leq N_i, i = 1, \ldots, n \\ & y_i \in \mathbb{Z}, i = 1, \ldots, n. \end{aligned} \tag{15}$$

The second case can be described as:

$$\begin{aligned} \underset{y}{\text{minimise}} \quad & \sum_{i}^{n} d_i \cdot H(y_i - y_{i,s}) \cdot (y_i - y_{i,s}) \\ \text{subject to} \quad & f\left(u_{\dot{W}_t}\right) \leq u_{max} \\ & 0 \leq y_i \leq N_i, i = 1, \ldots n \\ & y_i \in \mathbb{Z}, i = 1, \ldots, n. \end{aligned} \tag{16}$$

where $u_{\dot{W}_t}$ is the expected uncertainty of all the points of the representative experimental dataset, y_i is the number of sensors of type i, $y_{i,s}$ is the number of sensors of type i already in stock, N_i is the maximum allowable number of sensors of type i due to available space or other restrictions, d_i is the unitary cost of a sensor of type i, n is the size of the sensors database, H is the Heavyside step function, d_{max} is the maximum allowable cost, u_{max} is the maximum allowable uncertainty and f is a weight function for the uncertainty. A typical choice for f is the geometric mean of $u_{\dot{W}_t}$. As some kind of sensors are necessary (i.e., at least one mass flow rate transducer is needed), the value of the uncertainty can be defined as 100 % if the sum of all the sensors of that kind is equal to zero. As all general non-linear integral programming problems, both described situations are NP-hard, but some cases can be simplified. In the first case, when the uncertainty is to be minimised, if the test right designer has no sensors in stock, the constraints becomes linear and some efforts can be done into obtaining a better solving algorithm, as seen in [24]. Nevertheless, any NMIP algorithm may be used, such as a genetic algorithms [25] or branch and bound methods as described in [26] or, more recently, in [27] or [12].

The proposed algorithm to solve the problem is as follows:

- First, the relaxed non-integer problem is solved by means of sequential quadratic programming, giving results with low computational cost.
- Last, the ceilings and floors of the parameters are probed to get an approximation of the real optimum. The cost of this last stage is only $O(2^n)$ and gives better results than just rounding the result to the nearest integer.

Solving the relaxed non-integer problem with sequential quadratic programming usually gives results with less iterations than using other methods such as genetic algorithms. The authors have successfully used the SLSQP algorithm by D. Kraft [28] found in NLopt [29] and in SciPy [30], but other SQP algorithms may apply.

5. Application to a real case

The former methodology has been applied to a real testing campaign, computing uncertainties for the power output of an automotive turbine, giving the results shown in Figure 3, using a coverage factor of 3. The characteristics of the transducers used during the testing campaign are:

- Mass flow rate: one hot-film mass flow rate meter at the turbine outlet line, calibrated for air; maximum flow rate of 0.200 kg / s; expanded uncertainty of 1.1 % of the measured value for measurements higher than 0.005 kg / s, uniform distribution.
- Temperature: four type K thermocouples at the turbine inlet, other four at the outlet; expanded uncertainty of 1.52 K, including cable and acquisition system effects, uniform distribution.

- Pressure: two piezoresistive transducers at the turbine inlet and other two at the turbine outlet duct, with a maximum measurable absolute pressure of 0.5 MPa; expanded uncertainty of 12.5 hPa, uniform distribution.
- Humidity: one relative humidity sensor with a 5 % uncertainty, one thermistor with an uncertainty of 0.2 K and one piezoresistive transducer; expanded uncertainty of 3 hPa, uniform distribution.
- Duct diameter: one vernier calliper; expanded uncertainty of 0.02 mm, uniform distribution.

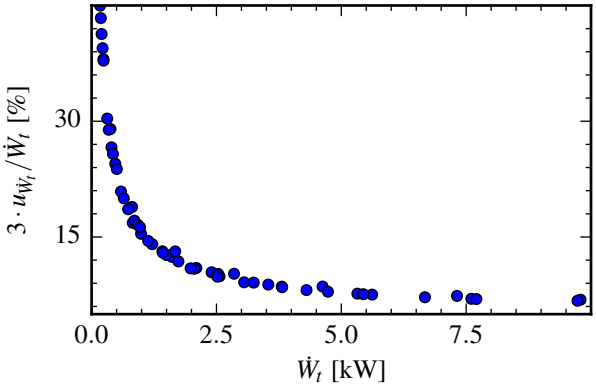

Figure 3: Typical power output uncertainty

In order to validate the results using the simplifications performed to compute Figure 3, Monte Carlo simulations were executed. The simulations were done for different power levels. For each experimental point, a high number of evaluations of the turbine power were done, each one modifying the measured variables with random values obtained from uniform distributions with expanded uncertainties equal to that given by the manufacturer's datasheets. The results for a low power point and a high power point and one million simulations are shown in figures 4 and 5, where the dashed line represents the simplified probability density function assumed in the former sections of the article and the solid one represents the normalized results of the Monte Carlo simulation. Also, the results for one thousand simulations are shown in figures 6 and 7.

The results of the simulations show almost no skewness and a bit less kurtosis than the simplified normal distribution, resulting in computed standard deviation comparable to that previously computed, as seen in figures 4, 5 and 10. Although the results of one thousand simulations give good results for standard deviation and mean, the form of the probability density function is distorted, as shown in figures 6 and 7. As can be seen in figures 8 and 9, a high number of evaluations is needed in order to properly compute higher order statistical moments such as skewness or kurtosis. The trade-off of several orders of magnitude in computational time makes the Monte Carlo simulations not viable for some applications, such as real time processing of test rig results. As the results for turbine output power uncertainty are the same using the linearised model and the Monte Carlo simulations, the former method will be used.

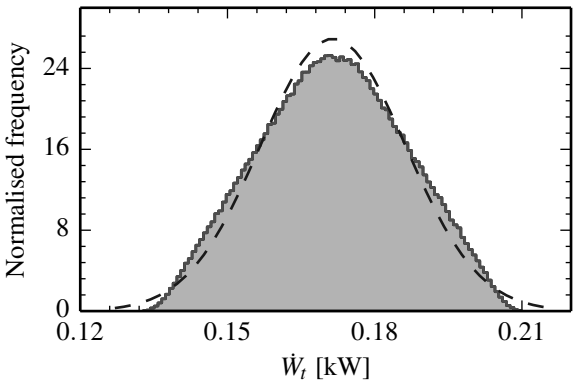

Figure 4: Monte Carlo simulation, low power, one million simulations

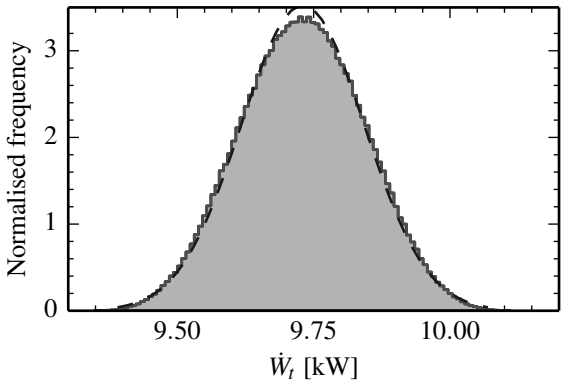

Figure 5: Monte Carlo simulation, high power, one million simulations

Figures 3 and 10 show big uncertainties at low turbine output powers. These results are due to measuring both small temperature differences between the inlet and the outlet of the turbine and small mass flow rates:

$$\lim_{\substack{\Delta T \to 0 \\ \dot{m} \to 0}} \frac{u_{\dot{W}_t}}{\dot{W}_t} \simeq \frac{u_{\hat{T}_3}^2 + u_{\hat{T}_4}^2}{\Delta T} \tag{17}$$

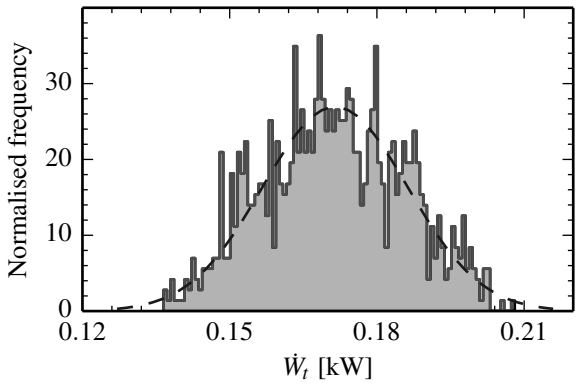

Figure 6: Monte Carlo simulation, low power, one thousand simulations

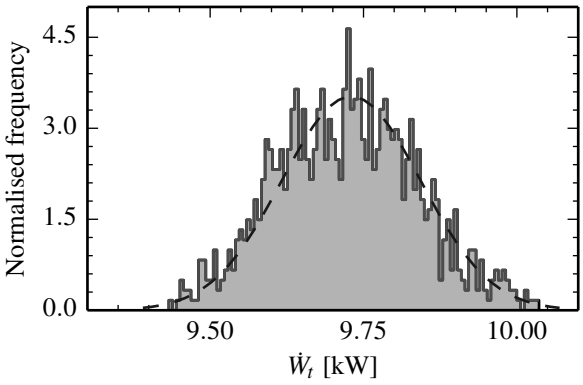

Figure 7: Monte Carlo simulation, high power, one thousand simulations

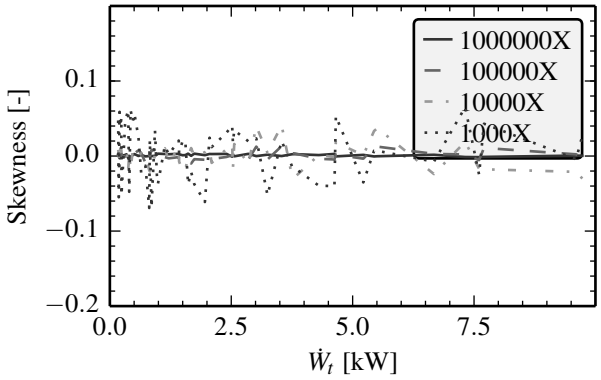

Figure 8: Monte Carlo simulation, skewness results for different number of evaluations

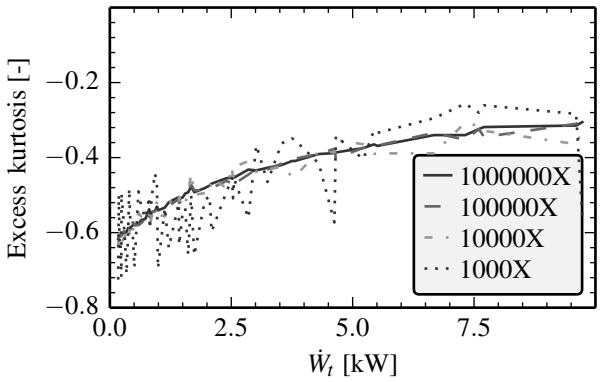

Figure 9: Monte Carlo simulation, kurtosis results for different number of evaluations

Equation 17 is valid only when the mass flow rate and the temperature drop is almost zero, but gives some insight in why very high uncertainties are expected when measuring low powers: changes in the inlet or outlet measured temperature of the order of the temperature transducer uncertainty translate in large changes in the computed turbine power if the temperature drop is comparable to the temperature transducer uncertainty.

At high powers, the expected uncertainty shows an asymptotic behaviour, ruled by the flow rate meter characteristics except in cases with low uncertainties associated to the mass flow rate measurement.

This dataset is used during an optimisation process for a new test rig with minimum uncertainty and the following results arise:

In figures 11 and 12, the optimisation has been done supposing no sensors in stock and minimising the uncertainty with increasing maximum costs. Figure 11 shows the geometric mean of the results and Figure 12 the uncertainty obtained at two different output power levels. In both figures only the transducer cost is shown, not taking into account other costs such as ducts or joints. The major improvements are found at low powers with relatively small costs, investing in better temperature sensors. In Figure 11, the first point is obtained with low cost mass flow rate sensors, one unshielded type K thermocouple per measurement section, low cost pressure transducers and no humidity measurement; the step 1 is obtained with one class B PT-100 transducer per measurement section and maintaining the same sensors as before; step 2 is obtained with 4 class A, 4 wire shielded PT-100 transducers per measurement section; in step 3, the mass flow rate sensor used has a lower uncertainty of 1 % of the measured value; step 4 introduces humidity sensors; step 5 is obtained with two low uncertainty mass flow rate sensors but reducing the number of tem-

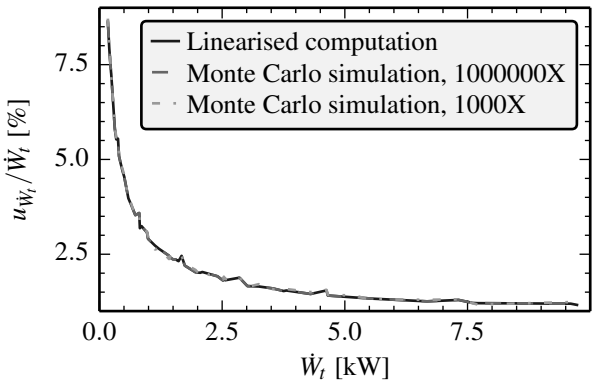

Figure 10: Monte Carlo simulation vs linearised model

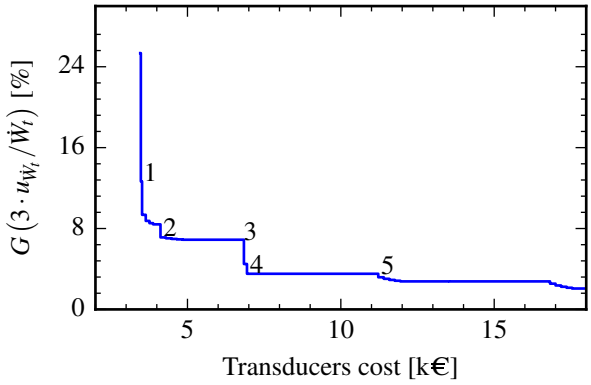

Figure 11: Results of an optimisation process

perature transducers; the rest of the optimisation is done with better mass flow rate sensors (the large steps in cost) and recovering temperature transducers up to the saturation point and investing in better pressure transducers (the smaller steps).

6. Conclusions

Turbine power uncertainties grow at a very fast rate when low powers are to be measured. The most important contributions are that derived of temperature measurement at the inlet and the outlet. When high accuracy in turbine power measurement is wanted, special care is needed in the thermocouples arrangement. Better results are expected by using lower uncertainty sensors, such as RTDs. When using the best measurement techniques available for temperature and mass flow rate, the effects of humidity and pressure become to be of importance.

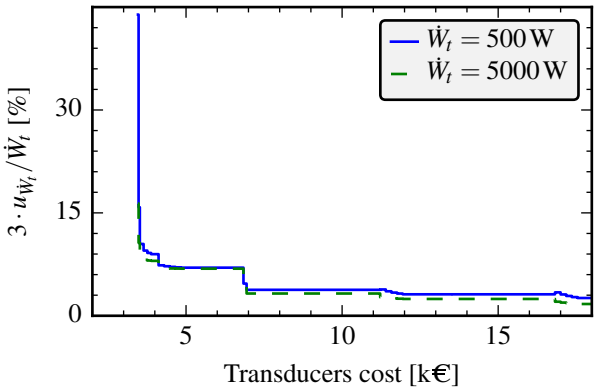

Figure 12: Results of an optimisation process - comparison at two different power outputs

The authors conclude that the first way to improve current power measurement techniques in turbocharger test rigs is to focus on mass flow rate sensors at high mass flow rates and on temperature sensors arrangement and selection at low mass flow rates, but if a global optimisation of the test rig is required, the methodology explained in section 4 may give better results with lower costs by using a good transducers database and the expression derived in section 3.

Finally, in order to compute propagations, a simple linear approximation gives good results. Monte Carlo simulations, in the other hand, give not only the uncertainty of the measurement but also the shape of the probability density function if a high number of evaluations are used, but at a computational cost several orders of magnitude higher, rendering this method unaffordable for real-time evaluation in gas stands. Nevertheless, they can be used for post-processing and sensor selection when more information than the mean and the standard deviation is needed, such as skewness, kurtosis or higher order moments.

7. Acknowledgements

This work has been partially supported by the Spanish Ministerio de Ciencia e Innovación through grant number DPI2010-20891-C02-02 and by the Spanish Ministerio de Economía y Competitividad through grant number TRA2012-36954.

Nomenclature

Symbols.

A Duct area

c Speed

c_p Specific heat capacity

d Cost

e Recovery factor

G Geometric mean

$\dot{m}$ Mass flow rate

N Maximum allowable number of sensors

p Pressure

H Heavyside's step function

R Gas constant

T Temperature

$\hat{T}$ Measured temperature

u Uncertainty

$\dot{W}_T$ Turbine power

Y Specific humidity

γ Specific heat capacity ratio

k Coverage factor

x Measured quantity

y Number of sensors of a given type

z Derived quantity

Subscripts.

3 Turbine inlet

4 Turbine outlet

0 Stagnation quantity

initial Initial quantity

M Maximum quantity

mean Mean quantity

s Available in stock

References

[1] J. M. Luján, V. Bermúdez, J. R. Serrano, C. Cervelló, Test bench for turbocharger groups characterization, SAE International (2002-01-0163).

[2] Turbocharger gas stand test code, S. of Automotive Engineers Inc (SAE J1826).

[3] A. Hajilouy-Benisi, M. Rad, M. Shahhosseini, Empirical assessment of the performance characteristics in turbocharger turbine and compressor, Experimental Techniques 34 (2010) 54–67.

[4] H. Montar, P. Chesse, D. Chalet, Describing uncertainties encountered during laboratory turbocharger compressor tests, Experimental Techniquesdoi:10.1111/j.1747-1567.2011.00734.x.

[5] A. M. AI-Qutub, F. A. AI-Sulaiman, Instrumentation design and uncertainty analysis for performance test of small centrifugal compressors, Proceedings of ASME Turbo Expo 2004 (GT2004-53828).

[6] P. Podevin, A. Clenci, G. Descombes, Influence of the lubricating oil pressure and temperature on the performance at low speeds of a centrifugal compressor for an automotive engine, Applied Thermal Engineering 31 (2-3) (2011) 194–201. doi:10.1016/j.applthermaleng.2010.08.033.

[7] J. R. Serrano, P. Olmeda, A. Pez, F. Vidal, An experimental procedure to determine heat transfer properties of turbochargers, Measurement Science and Technology 21 (3) (2010) 035–109. doi:10.1088/0957-0233/21/3/035109.

[8] T. Thurnheer, D. Edenhauser, P. Soltic, D. Schreiber, P. Kirchen, A. Sankowski, Experimental investigation on different injection strategies in a heavy-duty diesel engine: Emissions and loss analysis, Energy Conversion and Management 52 (1) (2011) 457–467. doi:10.1016/j.enconman.2010.06.074.

[9] M. Tancrez, J. Galindo, C. Guardiola, P. Fajardo, O. Varnier, Turbine adapted maps for turbocharger engine matching, Experimental Thermal and Fluid Science 35 (1) (2011) 146–153. doi:10.1016/j.expthermflusci.2010.07.018.

[10] P. Günther, F. Dreier, T. Pfister, J. Czarske, T. Haupt, W. Hufenbach, Measurement of radial expansion and tumbling motion of a high-speed rotor using an optical sensor system, Mechanical Systems and Signal Processing 25 (1) (2011) 319–330. doi:10.1016/j.ymssp.2010.08.005.

[11] W. Zhang, G. Xie, D. Zhang, Application of an optimization method and experiment in inverse determination of interfacial heat transfer coefficients in the blade casting process, Experimental Thermal and Fluid Science 34 (8) (2010) 1068–1076. doi:10.1016/j.expthermflusci.2010.03.009.

[12] D. Yokoya, T. Yamada, A mathematical programming approach to the construction of BIBDs, International Journal of Compututer Mathematics 88 (5) (2011) 1067–1082. doi:10.1080/00207160.2010.492869.

[13] N. P. Sahoo, M. P. Biswal, Computation of a multi-objective production planning model with probabilistic constraints, International Journal Of Computer Mathematics 86 (1) (2009) 185–198. doi:10.1080/00207160701734207.

[14] P. Pal, C. Das, A. Panda, A. Bhunia, An application of real-coded genetic algorithm (for mixed integer non-linear programming in an optimal two-warehouse inventory policy for deteriorating items with a linear trend in demand and a fixed planning horizon), International Journal of Computer Mathematics 82 (2) (2005) 163–175. doi:10.1080/00207160412331296733.

[15] W. D. Rose, Optimizing experimental design for coupled porous media flow studies, Experimental Thermal and Fluid Science 3 (6) (1990) 613–622. doi:10.1016/0894-1777(90)90078-L.

[16] Evaluation of measurement data – Guide to the expression of uncertainty in measurement (september 2008).

[17] D. Baroudi, E. Thibert, An instrumented structure to measure avalanche impact pressure: Error analysis from monte carlo simulations, Cold Regions Science and Technology 59 (2-3) (2009) 242 – 250, international Snow Science Workshop (ISSW) 2008. doi:10.1016/j.coldregions.2009.05.010.

[18] F. Payri, J. R. Serrano, P. Olmeda, A. Pez, F. Vidal, Experimental Methodology to Characterize Mechanical Losses in Small Turbochargers, in: Proceedings of the ASME Turbo Expo 2010, Vol. 5, Int Gas Turbine Inst, ASME, Glasgow, Scotland, 2010, pp. 413–423. doi:10.1115/GT2010-22815.

[19] J. R. Serrano, P. Olmeda, A. Tiseira, L. M. García-Cuevas, A. Lefebvre, Theoretical and experimental study of mechanical losses in automotive turbochargers, Energy 55 (0) (2013) 888–898. doi:10.1016/j.energy.2013.04.042.

[20] D. Bohn, N. Moritz, M. Wolff, Conjugate Flow and Heat Transfer Investigation of a Turbo Charger: Part II Experimental Results, in: Proceedings of the ASME Turbo Expo 2003, Vol. 3, ASME, Atlanta, Georgia, USA, 2003, pp. 723–729. doi:10.1115/GT2003-38449.

[21] J. R. Serrano, P. Olmeda, F. J. Arnau, M. Ángel Reyes Belmonte, A. Lefebvre, Importance of Heat Transfer Phenomena in Small Turbochargers for Passenger Car Applications, SAE Int. J. Engines 6(2) (2013) 716–728. doi:10.4271/2013-01-0576.

[22] J. Laverre, M. Pletin, The recovery factor of thermocouples placed in a subsonic flow, L'Aeronautique et L'Astronautique 58 (1976) 79–86.

[23] J. B. Esgar, A. L. Lea, Determination and use of the local recovery factor for calculating the effectiveness gas temperature for turbine blades, Tech. Rep. NACA-RM-E51G10, National Advisory Committee for Aeronautics (1951).

[24] M. Jünger, T. Liebling, D. Naddef, G. Nemhauser, W. Pulleyblank, G. Reinelt, G. Rinaldi, L. Wolsey, 50 Years of Integer Programming 1958–2008: The Early Years and State-of-the-Art Surveys, 2009. arXiv:arXiv:0906.5171v1.

[25] T. Yokota, M. Gen, Y.-X. Li, Genetic algorithm for nonlinear mixed integer programming problems and its applications, Computers and Industrial Engineering 30 (4) (1996) 905–917. doi:10.1016/0360-8352(96)00041-1.

[26] O. K. Gupta, A. Ravindran, Branch and Bound Experiments in Convex Nonlinear Integer Programming, Management Science 31 (12) (1985) 1533–1546. doi:10.1287/mnsc.31.12.1533.

[27] P. Bonami, J. Lee, S. Leyffer, A. Wchter, More Branch-and-Bound Experiments in Convex Nonlinear Integer Programming, http://www.optimization-online.org/DB_HTML/2011/09/3191.html (2011).

[28] D. Kraft, D. F. und Versuchsanstalt für Luft-und Raumfahrt Köln, A software package for sequential quadratic programming, Forschungsbericht / Deutsche Forschungs- und Versuchsanstalt für Luft- und Raumfahrt, Dt. Forschungs- u. Versuchsanst. für Luft- u. Raumfahrt (DFVLR), 1988.
URL http://books.google.es/books?id=1Di-ZwEACAAJ

[29] S. G. Johnson, The NLopt nonlinear-optimization package, "http://ab-initio.mit.edu/nlopt", last visited on 2013/09/25 (2007–).

[30] E. Jones, T. Oliphant, P. Peterson, et al., SciPy: Open source scientific tools for Python, "http://www.scipy.org/", last visited on 2013/09/25 (2001–).